A Wireless sEMG-Based Body-Machine Interface for Assistive Technology Devices

Article *in* IEEE Journal of Biomedical and Health Informatics · December 2016

DOI: 10.1109/JBHI.2016.2642837

8 authors, including:


C. L. Fall
Laval University


Gabriel Gagnon-Turcotte
Laval University


Alexandre Campeau-Lecours
Laval University


Clément Gosselin
Laval University

A Wireless sEMG-Based Body-Machine Interface for Assistive Technology Devices

C. L. Fall, *Student Member, IEEE*, G. Gagnon-Turcotte, *Student Member, IEEE*,
J. F. Dubé, J. S. Gagné, Y. Delisle, A. Campeau-Lecours, *Member, IEEE*,
C. Gosselin, *Fellow, IEEE,* and B. Gosselin, *Member, IEEE*

***Abstract*—Assistive Technology (AT) tools and appliances are being more and more widely used and developed worldwide to improve the autonomy of people living with disabilities and ease the interaction with their environments. This paper describes an intuitive and wireless surface electromyography (sEMG) based body-machine interface for AT tools. Spinal cord injuries (SCIs) at C5-C8 levels affect patients' arms, forearms, hands and fingers control. Thus, using classical AT control interfaces (keypads, joysticks, etc.) is often difficult or impossible. The proposed system reads the AT users' Residual Functional Capacities (RFCs) through their sEMG activity, and converts them into appropriate commands using a threshold-based control algorithm. It has proven to be suitable as a control alternative for assistive devices and has been tested with the JACO arm, an articulated assistive device of which the vocation is to help people living with upper-body disabilities in their daily life activities. The wireless prototype, the architecture of which is based on a 3-channel sEMG measurement system and a 915-MHz wireless transceiver built around a low-power microcontroller, uses low-cost off-the-shelf commercial components. The embedded controller is compared with JACO's regular joystick-based interface, using combinations of forearm, pectoral, masseter and trapeze muscles. The measured index of performance values are 0.88, 0.51 and 0.41 bits/s respectively, for correlation coefficients with the Fitt's model of 0.75, 0.85 and 0.67. These results demonstrate that the proposed controller offers an attractive alternative to conventional interfaces, such as joystick devices, for upper-body disabled people using assistive technologies such as JACO.**

***Index Terms*—Assistive Technologies, Assistive interfaces, gesture-based controller, surface electromyography (sEMG), body-computer interactions**

I. INTRODUCTION

Quality of Life (QoL) has become a priority for public health systems worldwide, while life satisfaction among people living with disabilities has also improved due to efforts in infrastructures, services and therapy, and advances in biomedical and rehabilitation engineering. Smart devices for rehabilitation represent a huge step forward in creating favourable living conditions for persons with disabilities [1]. Powered wheelchairs [2], smart prostheses [3], dedicated assistive robotic tools for therapy and assistance [4] are powerful Extrinsic Enablers (EE) that increase the life autonomy of their users [5].

Assistive technologies (ATs) have been the source of considerable research efforts as they have a real impact on disabled patients' living comfort. In [5], the Human Activity Assistive Technology (HAAT) model is described as a four-component framework that represents the interaction between disabled people and their activity, using assistive devices, in a specific environment. Thus, the importance of a suitable human-technology interface is underlined with the idea of a decision making tree based on the HAAT components involved.

Unlike for AT appliances, the use of AT tools require specific skills depending on the interaction interface provided [6]. For people with spinal-cord injuries (SCIs), the most common available interfaces for ATs can be classified into two categories. The first group consists of mechanical or electromechanical interfaces, which includes mainly switch devices (such as head-mounted switches), dedicated keypads, mice, trackballs, joysticks, head and hand pointers, sip-and-puff tools, mouthsticks, Lip control systems etc [7], [8]. Even though such devices are non-invasive, they remain difficult to use for persons living with severe SCIs depending on their level of injury and remaining abilities. Thus, a significant number of patients have to rely on a second group of interfaces which include movement tracking or pattern recognition based devices, and bio-signals based systems (see Figure 1). Those human-machine interfaces (HMIs) provide comfort, intuitiveness, discretion and "non-invasivity", which makes them attractive. In [9], the head and shoulders positions are read using an intuitive inertial measurement unit (IMU) based controller to control a robotic arm wirelessly. The eye controlled systems described in [10], [11], facial expression based controllers [12] and intraoral tongue-computer interfaces [13], [14] are good examples of movement tracking or pattern recognition based systems as the eye movement and tongue motion are associated to predefined commands. HMIs based on bio-signals translation aim at improving the technology in terms of intuitiveness and ease of use as the human body's physiological state reflects, inter alia, a user's willingness to move. Another class of emerging HMIs are Brain-Computer Interfaces (BCIs) which are devices that use the patient's brain signals to directly interact with the external environment [15], [16]. Such systems were proven effective and stand as a spectacular reach. However, they can be extremely invasive and expensive [17]. In contrast, using surface electromyography (sEMG) offers a non-invasive, effective, intuitive and natural way to interact with environments for better comfort and ease of use [18].

sEMG has been largely studied over the past thirty years [19]-[22] as a means of control and diagnosis, and finds its application in several fields [23]. The electrical signals

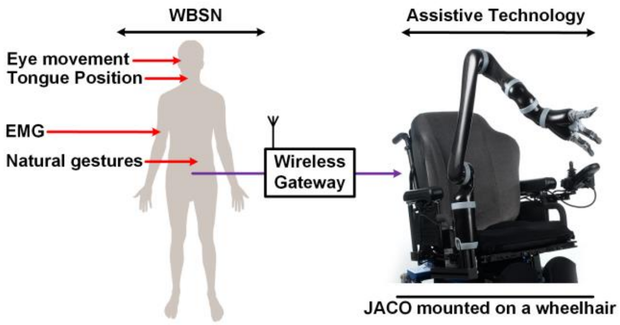

Fig. 1. Illustration of Wireless Body Sensor Networks (WBSN) based interfaces for people living with disabilities for them to control an assistive robotic device like the JACO arm [35].

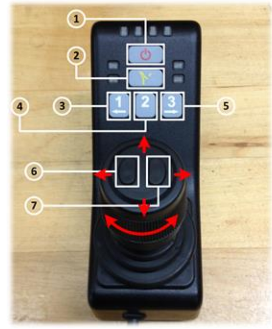

Fig. 2. JACO's joystick controller. Red arrow indicate the different possible positions of the stick, user buttons are numbered from 1 to 7.

generated by neuromuscular activities can be measured using non-invasive electrodes placed on the skin, over target muscles' innervation zones, and a dedicated bioinstrumentation system. HMIs based on these biological signals can be classified into 1) pattern recognition and 2) non pattern recognition based controller categories. Pattern recognition based controllers (PRBCs) are employed in diverse applications, from rehabilitation and gaming to human-robot interaction etc. [24]-[26]. These systems are able to identify a set of discriminant features, in time or frequency domain, from a small number of channels, using recognition algorithms based on linear discriminant analysis (LDA) [27], artificial neural networks (ANN) [28], neuro-fuzzy architectures [29], hidden Markov models (HMM) [30] and Gaussian mixture models (GMM) [31]. Then, the classifier's performance is quantified with an accuracy rate, usually above 90% [32]-[34]. Exoskeletons and intelligent prostheses are perfect examples of assistive devices that usually require the use of PRBCs and sEMG, the requirements in terms of intuitiveness are critical. However, the required computational resources for PRBCs lead to significant complexities in terms of implementation and power autonomy, which is often unsuitable for a low-cost and/or embedded controller solution. At the opposite, non-pattern recognition based controllers (NPRBCs), as described in [34], consist in finite state machines based approaches and onset detection algorithms. It is this second category of interface, also referred to as *amplitude based controllers* (ABCs) which is explored in this work. ABCs typically require lower implementation resources. In such a scheme, one or several thresholds are set for each EMG channel depending on a chosen criteria (raw amplitude, root-mean-square (RMS), energy …), using an appropriate detection technique [35], [36]. Specific control events are triggered anytime one or several thresholds are reached or whenever the amplitude criteria is within a specific range. The control algorithm activates the targeted degrees of freedom (DOFs) whose maximum number is determined by the number of channels available. Implementing more DOFs usually requires more sEMG channels, and a larger acquisition system, which can cause a loose in terms of comfort for the user.

Previously, the common trend has often been to work with resource demanding algorithms and powerful systems that are specialized for specific environments and fail to be useful in real application controlling standalone assistive technology (SAT), such as electrical wheelchairs or robotic arms. PRBCs are key to address the need of highly intuitive human-body interfaces, especially in the cases of prosthetic devices and exoskeletons, but are complex to design, implement and operate [37]. This complexity not helping, a gap had remained in the market for effective and convenient assistive technology devices. In fact, most SAT usually don't require such sophisticated controllers and complexity as only few discrete commands are necessary for control.

Besides, devices such as electrical wheelchairs or robotic arms can require the activation of several discrete commands and DOFs at once while default control means provided typically allow a maximum of only two DOFs at a time. Thus, for those devices, ABCs represent an excellent alternative to mechanical interfaces. For instance, JACO (see Figure 1) is a 5.7 kg lightweight 6-DOF serial robotic manipulator whose main application is to help people with upper-body disabilities to accomplish their daily living activities. The joints of JACO have unlimited rotation, which provides effective mobility and intuitiveness. The robot can be controlled using effector Cartesian coordinates or joint coordinates. Once mounted on an electrical wheelchair, its 6 DOFs as well as the 3 flexible fingers of the end-effector are controllable via the controller available on the wheelchair (joystick, sip-and-puff, chin, head or foot control) or alternative controllers such as *Penta* switches or mini-joysticks. People with upper body disabilities who use JACO reported concrete positive impacts on their everyday life [38]. The joystick-based controller can be individually adapted to each patient depending on their specific needs. However, in the case of severe disabilities, using such an interface can be tiring and difficult due to a lack of dexterity. For instance, people living with injuries around the C5-C8 cervical vertebrae may lose control of their wrists, hands and fingers and might not be able to hold or move objects on their own. Their residual functional capacities (RFCs) usually allow them to move their shoulders and to control their neck and masseter muscles properly [39]. Thus, using the sEMG signals of those parts of their body as a means of controlling a robotic arm like JACO could provide a more intuitive and easier control compared to a joystick based system.

This paper describes a wireless 3-DOF interface tool designed to be used by individuals living with upper body disabilities, such as arm or forearm amputations or SCI, depending on their RFCs, to facilitate their interactions with AT

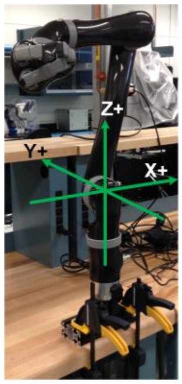

Fig. 3. Displacement of the JACO arm along axes X, Y, and Z corresponding to translations along the direction of vector $\vec{x}, \vec{y}$ or $\vec{z}$.

devices. The proposed controller offers a flexible and effective alternate solution through the use of sEMG compared to classical mec hanical and electromechanical control interfaces, which are often not accessible to severely impaired people. The proposed controller prototype focusses on simplicity and flexibility, in terms of algorithm design, hardware implementation, and wireless connectivity, while performing very well as demonstrated with the JACO arm, a commercial SAT application utilized by several end users. The main competitiveness of the proposed controller compared to the literature is the simplicity and flexibility of implementation and utilization, and its integration and validation within a commercial SAT application. Section II provides details on the methodology and the control algorithm used to design the proposed HMI. Section III describes the wireless prototyping platform employed to test the proposed controller while sections IV and V provide the performance measurements and conclusion.

II. Methodology and Control Algorithm

Joystick devices such as JACO's default controller provide a 3-axis translation (forward, backward, right and left inclinations, clockwise and anti-clockwise rotations) and up to 7 user buttons of which only 3 are necessary to fully control the robotic arm in real time (see Figure 2). Although it can be a sensitive and effective tool, target users often have difficulties to fully control the robotic arm since the manipulation of the joystick's handle can become complex and tiring.

Two groups of users are considered in this study (group A for people living with injuries around the C5-C8 cervical vertebrae and group B for persons who have forearm amputations). Thus, the sEMG-based HMI is designed to work with various target muscles, depending on patients' abilities. Since the JACO arm is used to test, at least 3 channels are necessary to provide a 3-axis translation as similar to the joystick interface. A wireless and simple design is crucial to meet the requirements in terms of comfort and ease of use. For electroencephalography (EEG) signals involved in BCI design, the causal relationship between a user's intent and his EEG pattern is not intuitive at first glance. Specific features are extracted from the raw signals before processing and classification, to confer a reliable classification scheme [40]. Depending on the chosen criteria, analyzing s EMG signals can be a lot easier and more intuitive. This work

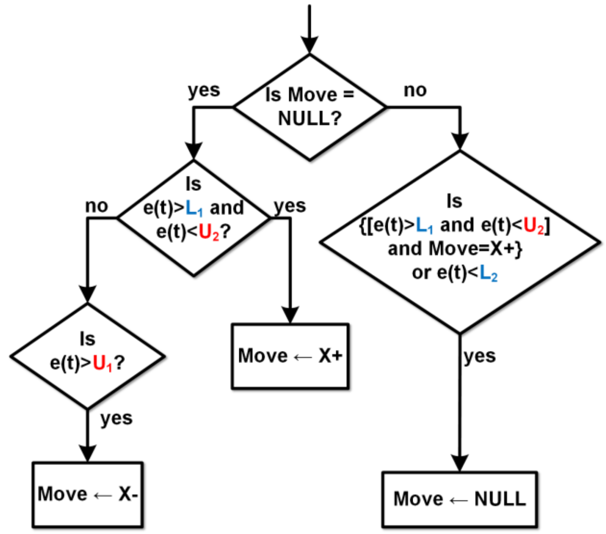

Fig. 4. Double-trigger mode illustration with an sEMG channel mapped to displacements on X. **e(t)** refers to the sEMG envelope signal as described in Section III.E and depicted in Figure 7. $\mathbf{L_1}$, $\mathbf{L_2}$, $\mathbf{U_1}$ and $\mathbf{U_2}$ are the lower and higher hysteresis thresholds' levels, respectively. **Move** is reported in figure 7.

employs an ABC to process the sEMG signals and control the JACO arm.

As mentioned, 3 sEMG channels are used to assess motion in the 3 Cartesian directions ($\vec{x}, \vec{y}, \vec{z}$) depicted in Figure 3 and, for ease of use, a dedicated software interface allows their dynamic mapping. A *positive displacement* along X axis (or Y, or Z) corresponds to a translation in the direction of vector $\vec{x}$ (or $\vec{y}$, or $\vec{z}$), while a *negative displacement* along any of the 3 axes correspond to a displacement in the opposite direction. Figure 4 describes the controller's behavior with a flow chart. The control algorithm proposed with the body-machine interface, referred to as the double- trigger mode, uses two hysteresis thresholds (one per allowed muscle contraction levels – low and high) for each channel to calculate the proper control output. The lower threshold corresponds to a lower level of muscle contraction and uses threshold levels L_1 and L_2 as depicted in Figure 4 and Figure 7. The higher hysteresis threshold, labeled of U_1 and U_2 in Figure 4 and Figure 7, corresponds to a higher level of contraction. The operator determines the threshold levels separately, based on the minimum and maximum values of the envelope during a lower or a higher contraction of the user. By default, activation of the higher hysteresis threshold triggers a negative displacement along the control axis, while activation of the lower threshold corresponds to a positive displacement (Fig. 4). Thereby, each control channel has 3 states: states 1 and 2 correspond to negative and positive displacements respectively, and state 0 defines the case when no significant sEMG activity is detected. More details and illustrative Figures (Figures 7 and 8) are provided on that topic in Section III.E. This strategy assumes that the user is able to perform two distinct levels of contractions that are tunable in case of fatigue, and repeat them over time, after calibration. Another type of control algorithm, the Pulse algorithm, is also used. In this method, channel states are triggered by pulse contractions. Although its implementation would be simple, this method may suffer from safety issues for utilization in real.

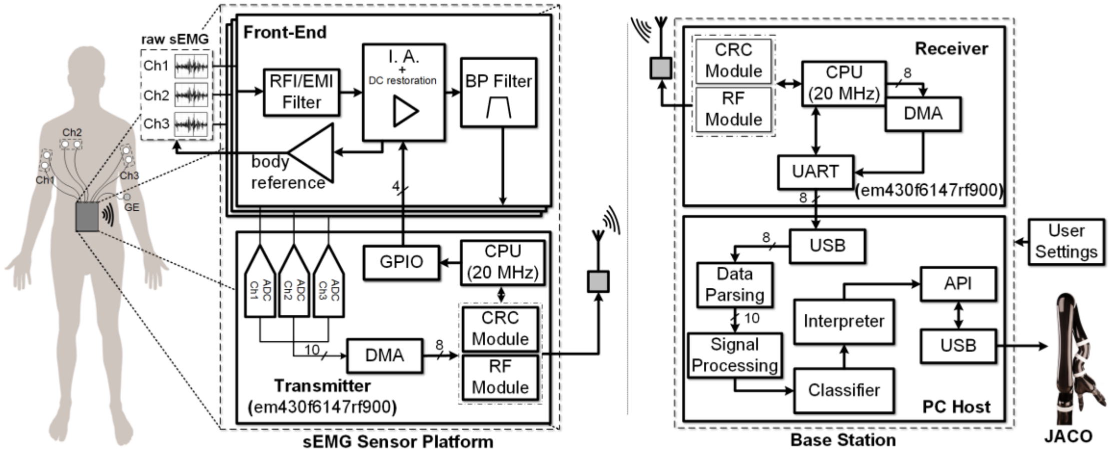

Fig. 5. Architecture diagram of the proposed interface.

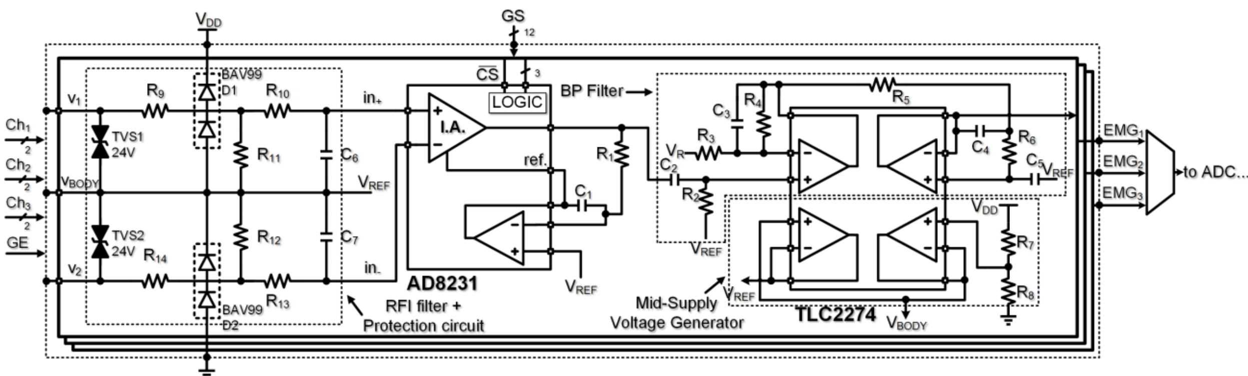

Fig. 6. Schematic of front-end circuit. The 3 sEMG channels are represented with their different connections (input channels (Ch_i), the ground electrode (GE) and gain select (GS) signals) and output signals (EMG_i).

Indeed in this mode, once a control action is triggered by a contraction, the user has no control until the next pulse contraction transpires.

The prototyping platform used to test the proposed sEMG amplitude based human-machine interface for upper-body disabled people is described in the next section.

III. The Wireless Platform Prototype

A. System overview

Figure 5 provides an overview of the wireless sEMG based interface prototype that has been implemented. Simplicity, low-cost, comfort and ease of use are among the most important features. The sensor platform was fixed around users' hips using a belt which provided comfort throughout the tests. Although much of the design effort have been dedicated towards the design of a practical and reliable control algorithm for patients, low-power design considerations have prevailed in the selection of integrated circuits and discrete components used in the implementation of the platform prototype and the firmware. For instance, power consumption is decreased through the utilization of an idle mode that is activated between analog-to-digital conversions to save energy. The following subsections describe the implemented platform prototype in detail, while the measured performance is presented in the next section.

B. The sEMG front-end circuit

A low-cost, efficient and non-invasive sensor architecture is necessary to confer a reliable control scheme for the proposed HMI. The instrumentation chain to collect sEMG signals is shown in more details in Figure 6 [41]. The front-end amplifier has 3 channels. It includes, an instrumentation amplifier with DC restoration providing differential inputs, a high common mode rejection ratio, a software selectable gain ranging from 1 to 128 V/V (AD8231, *Analog Device*), and a 20-Hz to 1000-Hz bandwidth band pass filter. To ensure user safety, high-voltage input protection circuits connected to the seven electrode leads (six differential inputs and one common ground electrode connected to the voltage reference) prevent damages that may result from electrostatic discharges or large input transient voltages. For noise performance, radio frequency interference (RFI) filters are used with the protection circuits and a DC restoration network with a cut-off frequency of 1.6 Hz is used to cancel the DC offset resulting from electrodes. After the signal is digitized, samples are transmitted to a remote PC host and transferable in real time into Matlab using an optional UDP communication. All measurements with the sensor prototype were performed using adhesive silver chloride electrodes. Although comfort issues might arise for long term patient usage, Ag/AgCl wet electrodes revealed to be stable throughout the measurements made in this wor k, and they are also very practical as noise artefacts are minimized compared to dry or

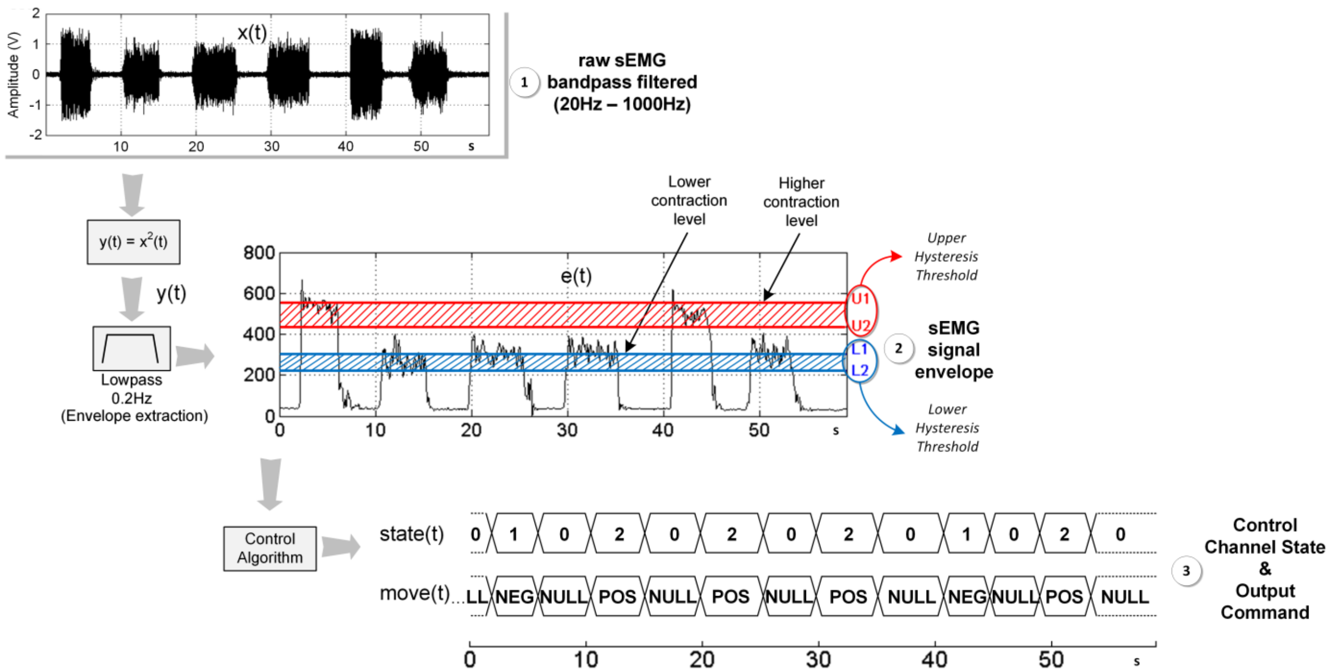

Fig. 7. sEMG signal processing and double-trigger algorithm control scheme. First the raw sEMG signal (1), *x(t)*, measured with the wireless prototyping platform described in II-B is filtered as described in III-E. *x(t)* is squared to obtain *y(t)* and the low-pass filter helps measuring the signal envelope *e(t)*, depicted in (2), which is translated into the right control channel state, *state(t)*, and the right output command, *move(t)*, depending on the hysteresis thresholds *(U1-U2)* and *(L1-L2)*, as detailed in II-B. NEG and POS stands for negative and positive displacement, respectively.

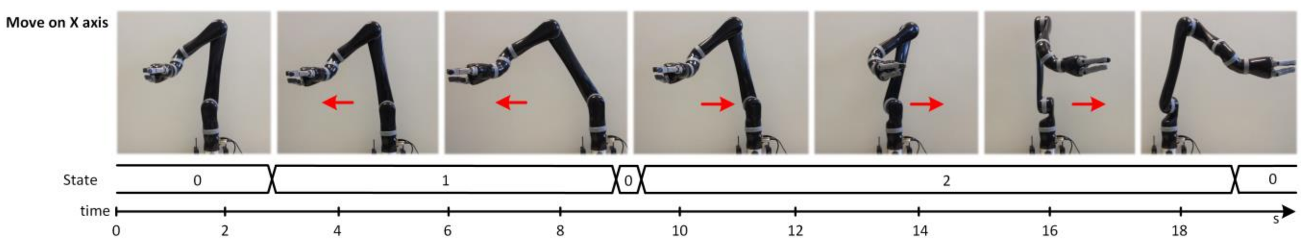

Fig. 8. Illustration of the control of JACO using the double trigger mode. The AT device is controlled along the X axis using one sEMG channel.

non-adhesive electrodes, even over long utilization periods. Thus, they were well indicated to accurately measure the controller performance.

C. *Low-power microcontroller and firmware design*

A development kit (em430f6147rf900, *Texas Instrument*) is used for prototyping the controller and the wireless transceiver. It features a system-on-chip (cc430f6147, *Texas Instruments*) which combines a low-power MSP430 microcontroller and a CC1101 sub-1-GHz RF transceiver. Digitization is performed using 3 analog input channels using the controller's 10 bits ADC at a sampling frequency at 2 kHz. The acquired data are buffered using the DMA module. In order to extend battery lifetime, the MCU is shut down during analog to digital conversions, consuming only 0.3 µA, and wakes up once all channels have been scanned, ensuring an efficient power consumption. Also, due to low power concerns, the sensor platform starts sending the measurement data only on demand, once the base station is connected to the PC host and the software interface (Section III.E) is initialized with the right acquisition parameters.

D. *Wireless transceiver*

The wireless communication is done using the aforementioned CC1101 sub-1-GHz RF module. The data acquired by the multi-channel sEMG front-end amplifier are used to construct a dedicated packet structure, which is fed to the transmitter, and then decapsulated and interpreted after reception. The RF transceiver performs a FSK-2 modulation using a 915 MHz carrier signal, resulting into an effective baudrate of 200 kbit/s. A 16-bit code redundancy check is also used to ensure data integrity, and a Clear Channel Assessment (CCA) detection improves data communications efficiency by preventing packet collisions when t he base station needs to transmit configuration data to the wireless sensor nodes. In fact, from the interface, the user initially sets the sensor's working parameters such as the number of channels to use and their respective gain (see Section III-B), and this information is sent via the base station transceiver board. A 1 byte ACK response from the sensor is then needed within 10ms and the transmission fails after 4 s of latency. A CP2102 uart-to-usb adapter from *Silicon Labs* connects the base station to the PC host at a serial baud rate of 460800 bits per second.

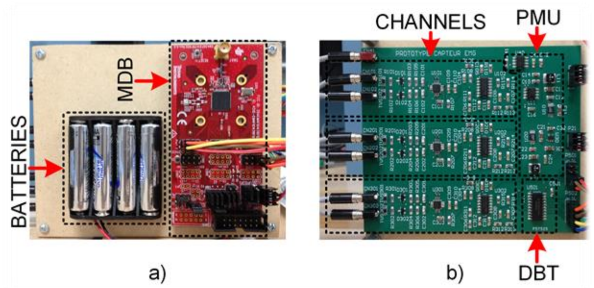

Fig. 9. The sEMG sensor node prototype. a) Top view of the 3-channel sensor showing batteries and the microcontroller development board (MDB), b) Bottom view of the prototype with the analog front-end channels outlined in dashed black, the dashed red box representing the power management unit (PMU) and the data bus transceiver (DBT) in yellow.

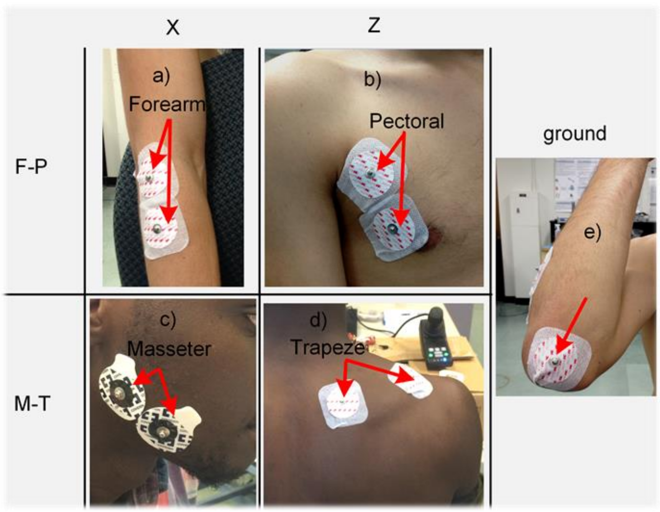

Fig. 10. Electrodes' placements over target muscles during tests. F-P = a) Forearm and b) Pectoral muscles, M-T = c) Masseter and d) Trapezes. The ground electrode's placement is also depicted in e). Displacements along X are done using forearm and masseter muscles, while translations along Z are trigger by pectoral and trapeze muscles contractions.

E. The user software interface and sEMG signals processing

Once sEMG signals have been measured and transmitted to the PC host by the wireless platform, a user software interface developed in C# allows the user to visualize the data. The program integrates JACO's software libraries and uses a dedicated API to communicate with the robotic arm and to provide its control and configuration data in proper format. First, data acquisition parameters, including the number of channels and their gains, can be selected by the user and sent to the wireless sEMG sensor node. The raw sEMG signal is band-pass filtered using a high-pass and a low-pass direct-form II biquad filters: the high-pass frequency is set to 20 Hz to reduce the impact of the DC offset in the analog circuits and the movement artefacts, while the low-pass frequency is set to 1000 Hz to pass sEMG signals, while increasing signal to noise ratio and avoiding aliasing. The resulting signal is squared, and pass to a 1^{st} order FIR low-pass filter of 0.2 Hz cut-off frequency to extract the envelope of the muscles activity (see Figure 7). Indeed, since time response is a critical parameter, FIR filtering is well suited for this application, and a 0.2-Hz cut-off frequency provides a good signal envelope for sEMG signals

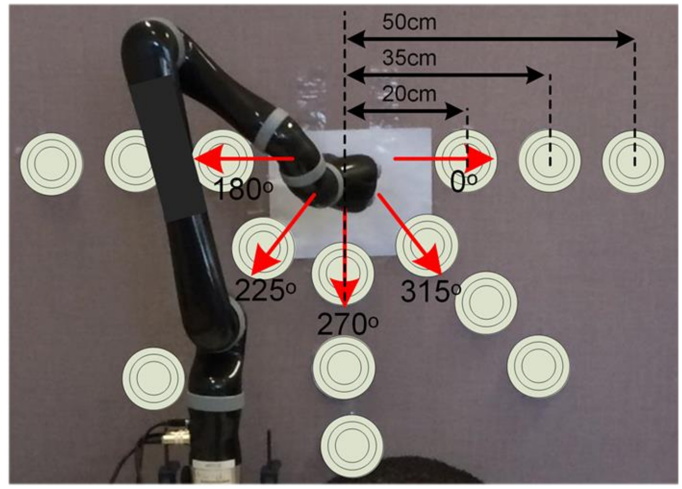

Fig. 11. Pointing task: The 3 different target dimensions are shown (4 cm, 8 cm and 10 cm) along the 5 different pointing angles (0°, 180°, 225°, 270° and 315°) at 3 different distances (20 cm, 35 cm and 50 cm). Targets are pinned on a board placed at 35 cm from JACO's fingers.

whose bandwidth lies between 20 and 1000 Hz. It is up to the user to define the right mapping of sEMG channels with the DOFs provided by the controlled AT (for example channels number 1, 2, and 3 associated with displacements on $\vec{x}$, $\vec{y}$ and $\vec{z}$ respectively by default for the JACO arm). The software interface allows to finely set the hysteresis thresholds (see Fig. 7), for any individual user to perform a proper control depending on his functionalities. The proposed controller is used as an alternative to the joystick to control the JACO arm. Thus, for each Cartesian axis, the output command consists of a constant speed parameter, whether positive of negative, to determine the direction of displacement that will occur. Thus, a simultaneous activation of the 3 DOFs can be performed according to the sEMG channels signal level, for performing motion along a diagonal, for instance. Figure 8 describes a 1-channel control sequence of the robotic arm, on the $\vec{x}$ axis, using the double trigger mode and showing the control channel's state (see section II.B). Also, JACO's specific parameters such as speed and velocity are selectable from the graphical user interface (GUI).

As the most important parameters in designing a HCI are functionality and usability [42], the controller has been tested by five able-bodied participants, using different target muscles to test efficiency for patients of group A and B, according to their RFCs. Results were compared to the use of the default joystick controller. The next section describes the measured performances and experimental results.

IV. Measured Performances

The wireless sEMG sensor prototyping platform measures 13x10 cm^2 and is designed to be used with wet Ag/AgCl electrodes with shielded leads and low-cost commercial off-the-shelf components. It is powered by 4 AAA Li batteries, which ensures a 22h autonomy (Figure 9).

As abovementioned, the control strategy (Section II) is based on the ability for the users to generate two distinct and repeatable myoelectric signals, in terms of average amplitude, for each target muscle. Five able-bodied subjects agreed to evaluate the comfort, intuitiveness and ease of use of the proposed interface, by performing several pointing tasks, and

TABLE I

MEAN POINTING TASK RESULTS USING THE JOYSTICK CONTROLLER

		A[1] = 200			**A = 350**			**A = 350**			[mm]
		W[2] = 40	**W = 80**	**W = 100**	**W = 40**	**W = 80**	**W = 100**	**W = 40**	**W = 80**	**W = 100**	[mm]
Pointing Angles	**0°**	4.47	1.20	1.52	3.81	3.77	2.17	3.74	3.12	4.82	
	180°	2.36	1.45	1.35	3.77	2.81	3.25	4.21	3.63	5.51	
	225°	3.21	1.84	2.09	4.81	4.81	3.60	4.33	4.33	4.50	[s]
	270°	4.12	1.61	1.70	2.95	4.09	2.82	3.68	3.37	3.61	
	315°	3.15	1.56	1.44	2.56	3.51	2.04	4.016	2.81	4.28	

[1] = pointing distance, [2] =target width

TABLE II

MEAN POINTING TASK RESULTS USING THE PROPOSED INTERFACE PROTOTYPE AND FOREARM AND PECTORAL MUSCLES

		A = 200			**A = 350**			**A = 350**			[mm]
		W = 40	**W = 80**	**W = 100**	**W = 40**	**W = 80**	**W = 100**	**W = 40**	**W = 80**	**W = 100**	[mm]
Pointing Angles	**0°**	5.70	3.00	3.60	5.65	5.37	4.83	6.48	5.87	7.12	
	180°	3.00	3.60	2.70	6.33	3.26	6.32	7.20	6.21	7.85	
	225°	4.15	2.90	4.55	7.00	6.30	5.23	7.64	7.58	7.23	[s]
	270°	6.32	3.40	3.00	6.15	6.00	3.70	7.42	7.02	6.45	
	315°	6.56	3.45	3.27	5.97	6.20	3.00	8.03	7.26	7.94	

TABLE III

MEAN POINTING TASK RESULTS USING THE PROPOSED INTERFACE PROTOTYPE AND FOR MASSETER AND TRAPEZE MUSCLES

		A = 200			**A = 350**			**A = 350**			[mm]
		W = 40	**W = 80**	**W = 100**	**W = 40**	**W = 80**	**W = 100**	**W = 40**	**W = 80**	**W = 100**	[mm]
Pointing Angles	**0°**	2.45	2.71	4.075	4.195	7.27	6.32	13.505	10.405	6.935	
	180°	3.90	4.06	3.645	5.845	4.665	4.415	5.745	6.585	6.38	
	225°	5.20	7.45	5.035	8.725	7.335	15.72	17.765	8.24	13.55	[s]
	270°	5.15	4.74	3.305	5.97	5.32	5.20	6.71	6.485	10.86	
	315°	2.79	4.55	3.97	6.83	6.6	7.505	10.095	12.925	8.215	

TABLE IV

POINTING TASK APPRECIATION SCORES

	USER 1	**USER 2**	**USER 3**	**USER 4**	**USER 5**
Joystick	1	1	1	1	1
F-P	4	3	2	4	2
M-T	3	4	4	5	5

F-P = Forearm and Pectoral muscles, M-T = Masseter and Trapeze muscles

Appreciation score: 1 = easy .. 5 = difficult

the results were compared with the robotic arm's joystick co ntroller (Figure 2). To demonstrate the efficiency for target users of group A (SCIs at C5-C8 levels), neck, masseter and trapeze muscle groups have been used, according to their RFCs. However, preliminary control tests revealed difficulty to use the neck muscle with the control algorithm implemented as a particular effort was often required to define two distinct contraction levels. In fact, although voluntary control was possible within a short time with these muscles, utilization over a long time period often caused discomfort. Therefore, the masseter and trapeze muscles, which are usually available for patients of group A, has been preferred for (see Fig. 10). For people living with arm or forearm amputation (group B), tests have been performed using wrist extensor muscles and pectoral zones (see Figures 10a and 10b). Participants were instructed on the controller's working principle and their ability to take control of the robotic arm were measured within a 2D pointing task whose procedure is described below. Two sEMG control channels were necessary to move JACO along X and Z axes (Fig. 3). Figure 11 shows electrode placements over the muscles groups and their mapping. For each channel, the calibration of the two thresholds needed to perform the control took 5 minutes and 35 seconds (5m35s) in average. Depending on users' trials, the operator had to set the proper values for hysteresis thresholds. This is visually done from the GUI that has been designed. Users particularly observed the complexity in determining the two contraction levels needed to perform the control, for each single channel. All protocols were performed in accordance with guidelines for ethical research at Laval University, and participants signed a written consent form.

A. Test procedures

The test procedure allowed for a 10-minutes user training phase for the test participants to familiarize with the proposed body-machine interface. During this training phase, test participants were allowed to freely control the robotic device along the 2 axes (X and Z) and to prepare for the pointing task. After this short training phase, they reported appropriate readiness to interact with the interface, and strong repeatability with respect to the calibration of the threshold levels.

Users ability to point at objects using the JACO arm guided with the proposed controller was evaluated for 5 pointing angles (0, 180, 225, 270 and 315^{o}) (see Fig. 11). Circular targets with three different diameters (40, 80 and 100 mm) were pinned on a board placed at 35 cm from JACO's fingers, at 3 distances from its home base position (200, 350 and 500 mm) [43]. Participants were told to point at a specific target by the operator who timed all tasks durations, and participants gave appreciation scores from 1 to 5 (1 for easy and 5 for difficult) at end.

First, the joystick controller depicted in Fig. 2 has been used and the test results over the 5 participants are reported in Table I. Then, Table II presents test results when using the proposed interface with the forearm and pectoral (F-P) muscles. Finally,

$$r_{CTRL} = [(X_{225} + X_{315})/2] \,/\, [(X_0 + X_{180} + X_{270})/3], \quad (1)$$

where X_Ω is the average task duration over angle Ω

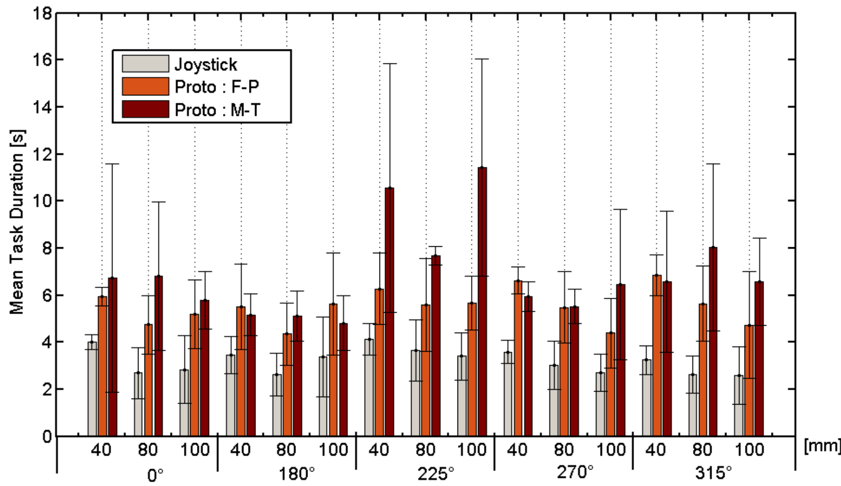

Fig. 12. Pointing task results over pointing angles.

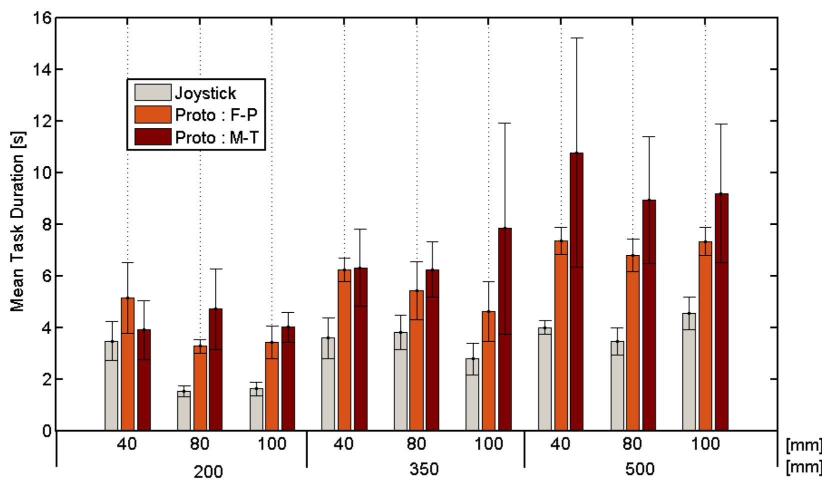

Fig. 13. Pointing task results over pointing distances.

Table III reports test results when the masseter and trapeze (M-T) muscles are used as control channels with the proposed interface. Figure 12 and 13 help visualizing task duration results overs the pointing angles and pointing distances respectively which are analyzed in Section IV.B.

The total times needed to perform all pointing tasks, calculated as a sum of all the 45 task duration times for each control method (see Table I, II and III), were 247.8 s and 309 s, when using the proposed controller with F-P and M-T muscles respectively, compared to 143.8 s for the joystick controller. For indication, the average appreciation scores were 3/5, 4.25/5 and 1/5, respectively (Table IV). Indexes of difficulty (IDs) were computed, according to Fitt's Law, from pointing distances and target diameters, and their corresponding mean p ointing task times. Experimentation results showed a good correlation with Fitt's model [44]. The regression coefficient *r* equals 0.85 for F-P muscles, 0.67 for M-T and 0.75 with the joystick device (see Figure 14) which shows relevance for Fitt's model representation, for index of performance (IPs) of 0.51, 0.41 and 0.88 bits/s, respectively. The section below provides comments and analysis of experimental results reported.

B. Performance analysis

The sEMG amplitude-based controller presented here is the result of investigation on alternate human-machine interfaces for assistive technologies, especially for the JACO arm. Evaluation results and a comparison with a joystick interface showed encouraging results and interesting research directions which have the potential to lead to significant improvements. A significant statistical concordance with Fitt 's model has been noticed. Task durations and IPs show that the proposed prototype is 1.66 times less efficient then the joystick device when used with F-P muscles, and 2.15 times less efficient when the JACO arm is controlled with M-T muscles. Regarding the pointing angles' influence on experiments, the maximum average times measured corresponds to 225° and 315° directions. In fact, ratios of results over those pointing angles with respect to other directions, calculated using (1), equal 1.089 and 1.4 when using the proposed prototype with F-P an d M-T muscle, respectively. It shows how more difficult it is on average to point at targets at 225° and 315°, compared to performances on other pointing angles (see Figure 12). As a comparison, this ratio decreases to 1.04 for the joystick

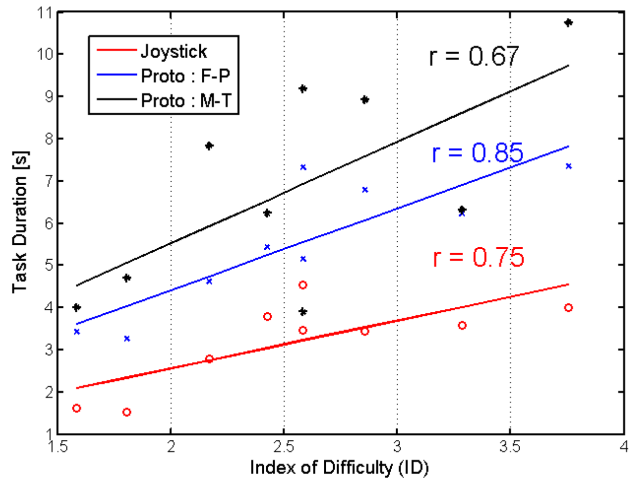

Fig. 14. Fitt's models with correlation coefficients for the joystick controller (red) and the proposed controller, both for the Forearm and Pectoral muscles (blue) and for the Masseter and Trapeze muscles (black).

controller. Since for those tasks users had to control the robotic device into both $\vec{x}$ and $\vec{z}$ axes, the experimental results reveal the increased complexity when it comes to focus on both sEMG controlling channels simultaneously. In fact, only 40% of the participants performed a synchronous control of JACO on both $\vec{x}$ and $\vec{z}$ directions while other users activated the 2 DOFs sequentially until they reached their targets. In [45], authors reported the same observation. According to appreciation scores, users found that using the joystick was 3 and 4.25 times less complicated than interacting with JACO through the proposed interface for the pointing tasks, using F-P and M-T muscles respectively. These results are acceptable somehow and shows how people who can't use mechanical interfaces like joysticks due to their disabilities could benefit from the proposed interface. In addition to the complexity in finding the two contraction levels during the calibration, we noticed that some participants suffered from fatigue after the tests, particularly on their forearm and masseter muscles, due to long contraction cycles. This could be improved by increasing the sensitivity of the analog front-end.

The proposed interface uses smart and robust threshold based algorithms and revealed good results and interesting directions for research. The choice of an ABC as an answer to the need of a low cost and simple design was a real challenge which has been addresses, as possibilities are limited compared to PRBCs. Future work will more focus on designing the proper sEMG based interface for people with no or very limited residual ability to use their upper limbs in order to reach more potential users. Although the proposed system has been tested with signals from forearm, biceps, pectoral, trapezes, neck and masseter muscles, which are usually available for a large category of users, we estimate that this controller has the flexibility to work wherever there is measurable electrical muscle activity on the body which can be voluntarily elicited by the user. Tests revealed that the performance does depend on the chosen target muscles, as shown in Section IV.A, but the system can be optimized and can adapt to a wide range of people by adjusting the threshold levels according to the user's target muscle type and signal strength.

V. Conclusion

In this paper, a sEMG-based ABC interface for assistive devices has been presented. The target users of such a technology are people living with severe upper-body disabilities that are totally or partially limited to the use of classical interfaces for assistive technologies. We tested the proposed controller with able-bodied users using masseter and shoulder muscles, which are usually available for people living with injuries situated around the C5 and C8 vertebrae. Using the forearm and pectoral muscles also revealed good performance and a promising alternative for people who have had their arm or forearm amputated or congenital limitations, such as the system described in [46]. The entire system has been described and the measure d performance has been reported as well. Fitt's model has been used as a measurement tool and tests with five able-bodied subjects have shown that the proposed sEMG controller has the potential to facilitate and improve JACO's control compared to the use of the joystick, exclusively, for people living with severe disabilities. Increasing the number of degrees of freedom of the controller remains an open challenge. In future work, the control strategy as well as the complete hardware and software architectures will be further improved for better comfort and precision control. As example, inertial measurement units are being combined with sEMG signals to improve performance.

References

[1] Steven W. Brose, Douglas J. Weber, Ben A. Salatin, Garret G. Grindle, Hongwu Wang, Juan J. Vazquez, and Rory A. Cooper. "The Role of Assistive Robotics in the Lives of Persons with Disability." *American Journal of Physical Medicine & Rehabilitation / Association of Academic Physiatrists* 89, no. 6 (June 2010): 509–21.

[2] M. Henderson, S. Kelly, R. Horne, M. Gillham, M. Pepper, and J.-M. Capron. "Powered Wheelchair Platform for Assistive Technology Development." In *2014 Fifth International Conference on Emerging Security Technologies (EST)*, 52–56, 2014.

[3] A.H. Al-Timemy, G. Bugmann, J. Escudero, and N. Outram. "Classification of Finger Movements for the Dexterous Hand Prosthesis Control With Surface Electromyography." *IEEE Journal of Biomedical and Health Informatics* 17, no. 3 (May 2013): 608–18.

[4] Shuai Zhang, S.I. McClean, C.D. Nugent, M.P. Donnelly, L. Galway, B.W. Scotney, and I. Cleland. "A Predictive Model for Assistive Technology Adoption for People With Dementia." *IEEE Journal of Biomedical and Health Informatics* 18, no. 1 (January 2014): 375–83.

[5] Albert M. Cook, and Janice Miller Polgar. "Cook and Hussey's Assistive Technologies: Principles and Practice." Elsevier Health Sciences, 2013.

[6] Albert M. Cook, and Janice Miller Polgar. *Essentials of Assistive Technologies*. Elsevier Health Sciences, 2014.

[7] Jacob O. Wobbrock, and Krzysztof Z. Gajos. "Goal Crossing with Mice and Trackballs for People with Motor Impairments: Performance, Submovements, and Design Directions." *ACM Trans. Access. Comput.* 1, no. 1 (May 2008).

[8] Jose M. Archajo, and R. de Deus Lopes. "Human-Computer Interface Controlled by the Lip." *IEEE Journal of Biomedical and Health Informatics* 19, no. 1 (January 2015): 302–8.

[9] C. L. Fall, P. Turgeon, V. Maheu, A. Lecours, M. Boukadoum, S.Roy, D. Massicotte, C. Gosselin, and B. Gosselin. "Intuitive Wireless Control of a Robotic Arm for Upper Body Disabled People," *The 37th Annual International Conference of the IEEE Engineering in Medicine and Biology Society* (EMBC'15), 4399 - 4402, 2015.

[10] Iestyn Jowers, Miquel Prats, Alison McKay, and Steve Garner. "Evaluating an Eye Tracking Interface for a Two-Dimensional Sketch Editor." *Computer-Aided Design* 45, no. 5 (May 2013).

[11] Jiaxin Ma, Yu Zhang, Yunjun Nam, A. Cichocki, and F. Matsuno. "EOG/ERP Hybrid Human-Machine Interface for Robot Control." In *2013 IEEE/RSJ International Conference on Intelligent Robots and Systems (IROS)*, 859–64, 2013.

[12] Zhen-Peng Bian, J. Hou, Lap-Pui Chau, and N. Magnenat-Thalmann. "Facial Position and Expression Based Human Computer Interface for Persons with Tetraplegia." *IEEE Journal of Biomedical and Health Informatics* PP, no. 99 (2015): 1–1.

[13] Hangue Park, M. Kiani, Hyung-Min Lee, Jeonghee Kim, J. Block, B. Gosselin, and M. Ghovanloo. "A Wireless Magnetoresistive Sensing System for an Intraoral Tongue-Computer Interface." *IEEE Transactions on Biomedical Circuits and Systems* 6, no. 6 (December 2012): 571–85.

[14] Xueliang Huo and Maysam Ghovanloo, "Evaluation of a wireless wearable tongue–computer interface by individuals with high-level spinal cord injuries," Journal of Neural Engineering, vol. 7, no. 2, p. 026008, 2010.

[15] José del R. Millán, Rüdiger Rupp, Gernot Mueller-Putz, Roderick Murray-Smith, Claudio Giugliemma, Michael Tangermann, Carmen Vidaurre, et al. "Combining Brain–computer Interfaces and Assistive Technologies: State-of-the-Art and Challenges." *Neuroprosthetics* 4 (2010): 161.

[16] M. Smith, K. Weaver, T. Grabowski, and F. Darvas. "Utilizing High Gamma (HG) Band Power Changes as a Control Signal for Non-Invasive BCI." In *Brain-Computer Interface Research*, edited by Christoph Guger, Brendan Z. Allison, and Günter Edlinger, 83–91. SpringerBriefs in Electrical and Computer Engineering. Springer Berlin Heidelberg, 2013.

[17] Eleanor A. Curran, and Maria J. Stokes. "Learning to Control Brain Activity: A Review of the Production and Control of EEG Components for Driving Brain–computer Interface (BCI) Systems." *Brain and Cognition* 51, no. 3 (April 2003): 326–36.

[18] M.V. Liarokapis, P.K. Artemiadis, K.J. Kyriakopoulos, and E.S. Manolakos. "A Learning Scheme for Reach to Grasp Movements: On EMG-Based Interfaces Using Task Specific Motion Decoding Models." *IEEE Journal of Biomedical and Health Informatics* 17, no. 5 (September 2013): 915–21.

[19] R. N. Scott, and P. A. Parker. "Myoelectric Prostheses: State of the Art." *Journal of Medical Engineering & Technology* 12, no. 4 (January 1, 1988).

[20] A. Hiraiwa, K. Shimohara, and Y. Tokunaga. "EMG Pattern Analysis and Classification by Neural Network." In *IEEE International Conference on Systems, Man and Cybernetics, 1989. Conference Proceedings*, 1113–1115 vol.3, 1989.

[21] K.R. Wheeler, M.H. Chang, and K.H. Knuth. "Gesture-Based Control and EMG Decomposition." *IEEE Transactions on Systems, Man, and Cybernetics, Part C: Applications and Reviews* 36, no. 4 (July 2006).

[22] Cinthia Itiki, Sergio S. Furuie, and Roberto Merletti. "Compression of High-Density EMG Signals for Trapezius and Gastrocnemius Muscles." *BioMedical Engineering OnLine* 13, no. 1 (March 10, 2014).

[23] Marco Barbero, Roberto Merletti, and Alberto Rainoldi. "Introduction and Applications of Surface EMG." In *Atlas of Muscle Innervation Zones*, 3–6. Springer Milan, 2012.

[24] Ping Zhou, and Xu Zhang. "A Novel Technique for Muscle Onset Detection Using Surface EMG Signals without Removal of ECG Artifacts." *Physiological Measurement* 35, no. 1 (January 1, 2014): 45.

[25] D. Yang, W. Yang, Q. Huang, and H. Liu. "Classification of Multiple Finger Motions during Dynamic Upper Limb Movements." *IEEE Journal of Biomedical and Health Informatics*, no. 99 (2015): 1–1.

[26] E. Scheme, B. Lock, L. Hargrove, W. Hill, U. Kuruganti, and K. Englehart. "Motion Normalized Proportional Control for Improved Pattern Recognition-Based Myoelectric Control." *IEEE Transactions on Neural Systems and Rehabilitation Engineering* 22, no. 1 (January 2014): 149–57.

[27] Zhijun Li, Baocheng Wang, Fuchun Sun, Chenguang Yang, Qing Xie, and Weidong Zhang. "sEMG-Based Joint Force Control for an Upper-Limb Power-Assist Exoskeleton Robot." *IEEE Journal of Biomedical and Health Informatics* 18, no. 3 (May 2014): 1043–50.

[28] G. R. Naik, and H. T. Nguyen. "Nonnegative Matrix Factorization for the Identification of EMG Finger Movements: Evaluation Using Matrix Analysis." *IEEE Journal of Biomedical and Health Informatics* 19, no. 2 (March 2015): 478–85.

[29] M. Khezri, M. Jahed, and N. Sadati. "Neuro-Fuzzy Surface EMG Pattern Recognition For Multifunctional Hand Prosthesis Control." In *IEEE International Symposium on Industrial Electronics, 2007. ISIE 2007*, 269–74, 2007.

[30] A. D. C. Chan, and K. B. Englehart. "Continuous Myoelectric Control for Powered Prostheses Using Hidden Markov Models." *IEEE Transactions on Biomedical Engineering* 52, no. 1 (January 2005): 121–24.

[31] Yonghong Huang, K. B. Englehart, B. Hudgins, and A. D. C. Chan. "A Gaussian Mixture Model Based Classification Scheme for Myoelectric Control of Powered Upper Limb Prostheses." *IEEE Transactions on Biomedical Engineering* 52, no. 11 (November 2005): 1801–11.

[32] G.R. Naik, A. Acharyya, and H.T. Nguyen. "Classification of Finger Extension and Flexion of EMG and Cyberglove Data with Modified ICA Weight Matrix." In *2014 36th Annual International Conference of the IEEE Engineering in Medicine and Biology Society (EMBC)*, 3829–32, 2014.

[33] Kexin Xing, Peipei Yang, Jian Huang, Yongji Wang, and Quanmin Zhu. "A Real-Time EMG Pattern Recognition Method for Virtual Myoelectric Hand Control." *Neurocomputing*, January 10, 2014.

[34] Asghari Oskoei, Mohammadreza, and Huosheng Hu. "Myoelectric Control systems—A Survey." *Biomedical Signal Processing and Control* 2, no. 4 (October 2007): 275–94.

[35] M.B.I. Raez, M.S. Hussain, and F. Mohd-Yasin. "Techniques of EMG Signal Analysis: Detection, Processing, Classification and Applications." *Biological Procedures Online* 8 (March 23, 2006): 11–35.

[36] Aaron J. Young, Lauren H. Smith, Elliott J. Rouse, and Levi J. Hargrove. "A Comparison of the Real-Time Controllability of Pattern Recognition to Conventional Myoelectric Control for Discrete and Simultaneous Movements." *Journal of NeuroEngineering and Rehabilitation* 11, no. 1 (January 10, 2014): 5.

[37] J. L. Contreras-Vidal, A. Kilicarslan, H. Huang, and R. G. Grossman. "Human-centered design of wearable neuroprostheses and exoskeletons." *AI Mag. 36*, (2015).

[38] A. Campeau-Lecours, V. Maheu, S. Lepage, S. Latour, L. Paquet and N. Hardie. "JACO Assistive Robotic Device: Empowering People With Disabilities Through Innovative Algorithms." *2016 Rehabilitation Engineering and Assistive Technology Society of North America (RESNA) annual conference* (July 2016).

[39] William McKinley, Ajit B. Pai, and Udayan Kulkarni. "Functional Outcomes per Level of Spinal Cord Injury," July 27, 2015. http://emedicine.medscape.com/article/322604-overview.

[40] M. S. Al-Quraishi, A. J. Ishak, S. A. Ahmad, M. K. Hasan. "Impact of feature extraction techniques on classification accuracy for EMG based ankle joint movements," In *10th IEEE Asian Control Conference (ASCC)*, (pp. 1-5), 2015.

[41] A. Yousefian, S. Roy, and B. Gosselin. "A Low-power wireless multi-channel surface EMG sensor with simplified ADPCM data compression." *2013 IEEE International Symposium on Circuits and Systems (ISCAS)*, 2013.

[42] A.R. Mathew, A. Al Hajj, and A. Al Abri. "Human-Computer Interaction (HCI): An Overview." In *2011 IEEE International Conference on Computer Science and Automation Engineering (CSAE)*, 1:99–100, 2011.

[43] Outi Tuisku, Veikko Surakka, Toni Vanhala, Ville Rantanen, and Jukka Lekkala. "Wireless Face Interface: Using Voluntary Gaze Direction and Facial Muscle Activations for Human–computer Interaction." *Interacting with Computers* 24, no. 1 (January 2012): 1–9.

[44] Charles E. Wright, and Francis Lee. "Issues Related to HCI Application of Fitts's Law." *Human–Computer Interaction* 28, no. 6 (November 2, 2013): 548–78.

[45] M. R. Williams and R. F. Kirsch. "Evaluation of head orientation and neck muscle EMG signals as command inputs to a human–computer interface for individuals with high tetraplegia." In *IEEE Transactions on Neural Systems and Rehabilitation Engineering*, 16, no. 5 (2008): 485-496.

[46] Mei-Hua Lee, Rajiv Ranganathan, A. Florian Kagerer, and Ranjan Mukherjee. "Body-Machine Interface for Control of a Screen Cursor for a Child with Congenital Absence of Upper and Lower Limbs: A Case Report." *Journal of NeuroEngineering and Rehabilitation* 13 (2016).

Cheikh Latyr Fall (S'14) received his Master's degree in Automatic Control and Electrical Engineering from the Institut National des Sciences Appliquées (INSA) of Toulouse, France, in 2013. He is pursuing the Ph.D. degree in Electrical Engineering at the Biomedical Microsystems Laboratory, Laval

University, Quebec, Canada. His main research interests are assistive technologies, rehabilitation robotics, human-machine interfaces, wireless body sensor networks and biomedical instrumentation.

Gabriel Gagnon-Turcotte (S'14) received the B.Sc. degree in Computer Engineering from Laval University, Quebec, Canada, in 2014, and the M.Sc. degree in Electrical Engineering from Laval University, Quebec, Canada, in 2015. He is currently pursuing the Ph.D. degree in Electrical Engineering at the Biomedical Microsystems Laboratory, Laval University, Quebec, Canada. His main research interests are neural compression algorithms, wireless low-power biomedical systems, system-level digital design and VLSI signal processing.

Alexandre Campeau-Lecours (S'10-M'15) received the B.Eng. degree in Mechanical Engineering (mechatronics) from École Polytechnique de Montréal, Quebec, Canada, in 2008 and Ph.D. degree from Laval University, Quebec, Canada, in 2012. From 2012 to 2015, he worked in industry at Kinova as a research and development project manager in control and robotic algorithms. He is an assistant professor in the Department of Mechanical Engineering at Laval University since 2015. His main research interests focus on physical human-robot interaction, assistive technologies and intelligent robotic algorithms.

Clément Gosselin (S'88-M'89-F'13) received the B. Eng. degree in Mechanical Engineering from the Université de Sherbrooke, Québec, Canada, in 1985, and the Ph.D. degree from McGill University, Montréal, Québec, Canada in 1988.

He was then a post-doctoral fellow at INRIA in Sophia-Antipolis, France in 1988-89. In 1989 he was appointed by the Department of Mechanical Engineering at Université Laval, Québec where he is a Full Professor since 1997. He is currently holding a Canada Research Chair in Robotics and Mechatronics since January 2001. He was a visiting researcher at the RWTH in Aachen, Germany in 1995, at the University of Victoria, Canada in 1996 and at the IRCCyN in Nantes, France in 1999.

His research interests are kinematics, dynamics and control of robotic mechanical systems with a particular emphasis on the mechanics of grasping, the kinematics and dynamics of parallel manipulators and the development of human-friendly robots. His work in the aforementioned areas has been the subject of numerous publications in international journals and conferences as well as of several patents and two books. He has been directing many research initiatives, including collaborations with several Canadian and foreign high-technology companies and he has trained more than 100 graduate students. He is an Associate Editor of the IEEE Robotics and Automation Letters and of the ASME Journal of Mechanisms and Robotics.

Dr. Gosselin received several awards including the ASME DED Mechanisms and Robotics Committee Award in 2008 and the ASME Machine Design Award in 2013. He was appointed Officer of the Order of Canada in 2010 for contributions to research in parallel mechanisms and underactuated systems. He is a fellow of the ASME, of the IEEE and of the Royal Society of Canada.

Benoit Gosselin (S'02–M'08) obtained the Ph.D. degree in Electrical Eng. from École Polytechnique de Montréal in 2009, and he was an NSERC Postdoctoral Fellow at the Georgia Institute of Technology in 2010. He is currently an Associate Professor at the Depart. of ECE at Université Laval, where he is heading the Biomedical Microsystems Lab. His research interests include wireless microsystems for brain computer interfaces, analog/mixed-mode and RF integrated circuits for neural engineering, interface circuits of implantable sensors/actuators and point-of-care diagnostic microsystems for personalized healthcare.

Dr Gosselin is an Associate Editor of the *IEEE Transactions on Biomedical Circuits and Systems* and he is Chair and Founder of the Quebec IEEE CAS/EMB Chapter (2015 Best New Chapter Award). He served on the committees of several int'l conferences such as IEEE BIOCAS, IEEE NEWCAS, IEEE EMBC/NER, and IEEE ISCAS, and he currently serves on the committee of the IEEE NEWCAS'17. His research consists of developing innovative microelectronic platforms to collect and study brain activity through advanced multimodal bioinstrum-entation and actuation technology. In addition to earn several awards, such as the 2015 Mitacs Award for Outstanding Innovation and the IEEE BioCAS'15 Best paper Award, his contributions led to the commercialization of the first wireless bioelectronic implant to combine optogenetics and large-scale brain monitoring capabilities within a single device, with partner Doric Lenses Inc.

Jean-François Dubé photograph and biography not available at the time of publication

Jean Simon Gagné photograph and biography not available at the time of publication

Yanick Delisle photograph and biography not available at the time of publication